Properties of wood polymer composites based on polypropylene/olive wood flour: effects of fiber treatment and compatibilizer

Slim Souissi, Ferdaous Lachtar, Ahmed Elloumi, Anne Bergeret

Properties of wood polymer composites based on polypropylene/olive wood flour: effects of fiber treatment and compatibilizer

Slim Souissi[1] · **Ferdaous Lachtar**[1,2] · **Ahmed Elloumi**[1] · **Anne Bergeret**[2]

Abstract

In this study, wood polymer composites (WPC) were produced by polypropylene (PP) as the matrix material and 30 wt % olive wood flour (OWF) as the filler material, for injection applications. Various treatments of OWF—including single treat-ment or co-modifications using the silane treatment, heat treatment, and maleic anhydride grafted polypropylene (MAPP) compatibilizer—were used to improve PP/OWF compatibility and mechanical properties. Structural and thermal charac-terization of the OWF after treatment has been implemented using Fourier transform infrared spectroscopy (FTIR) and thermogravimetric analysis (TGA). FTIR and energy-dispersive X-ray (EDX) analyses revealed the interactions between OWF and silane coupling agent. Silane and heat treatments increased the thermal stability of OWF. Results of mechanical tests revealed that the OWF increased Young's modulus values of PP/OWF composites with respect to those of pure PP, while their tensile and impact strengths decreased. Moreover, heat and MAPP treatments enhanced the mechanical properties. Heat treatment introduced higher toughness in PP/OWF composites compared to the other treatments. Scanning electron microscopy (SEM) showed the evidence of the improved interfacial adhesion and consequently mechanical properties of the PP/OWF composites by the used treatments. A further enhancement in mechanical properties was recorded for these wood polymer composites with co-modifications of OWF with MAPP.

✉ Slim Souissi
slim.souissi@ymail.com

[1] Laboratory of Electromechanical Systems (LASEM), National Engineering School of Sfax, University of Sfax, 3038 Sfax, Tunisia

[2] Polymers Composites and Hybrids (PCH), IMT Mines Ales, Ales, France

Graphical Abstract

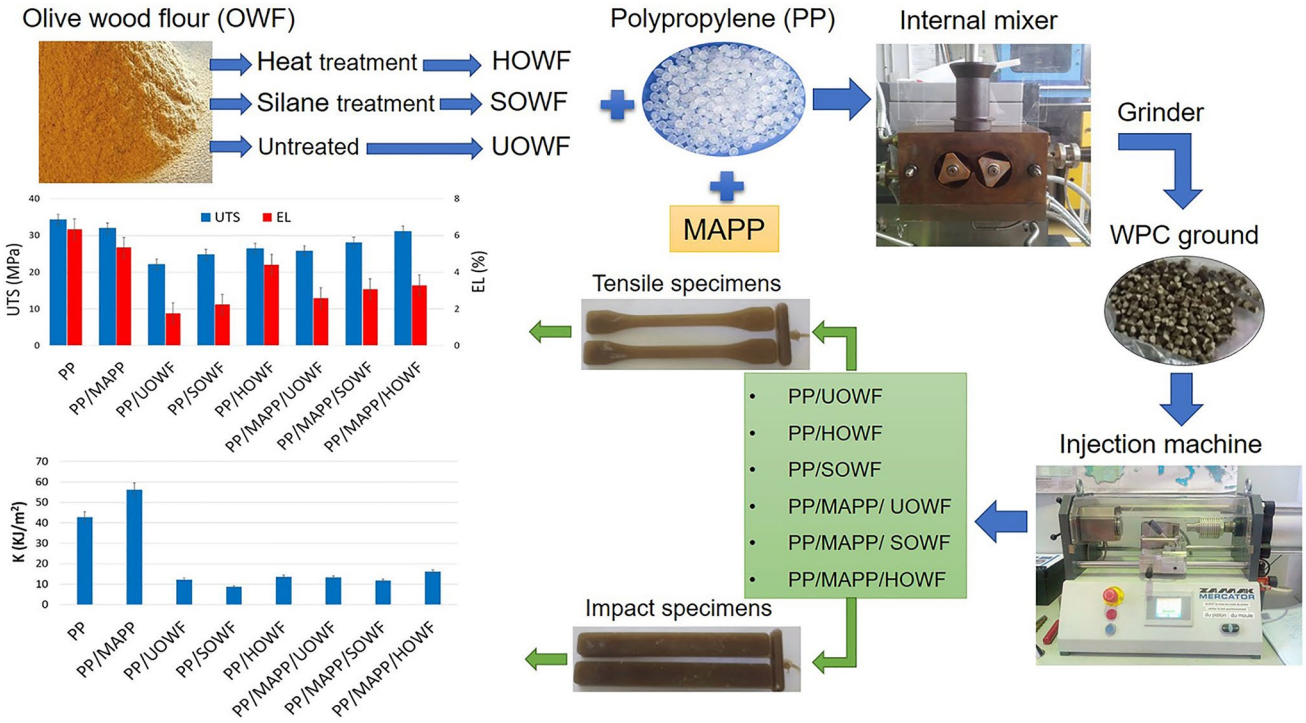

Keywords Wood polymer composite · Olive wood flour · Heat treatment · Silane treatment · MAPP · Mechanical properties

Introduction

Wood polymer composites (WPCs) have been drawing more and more interest over the last few years because of the strict environmental legislation for using plastics, lack of petroleum resources and the deforestation due to the excessive use of wood [1–3]. WPCs combine the desirable features of wood and plastics such as high mechanical properties, dimensional and thermal stabilities, wear resistance, and lower water absorption compared to wood [4]. This allows WPC to make progress in various fields including construction [5, 6] (outdoor decking, indoor furniture, window and door frames, parquet flooring), and transport applications uses [7, 8].

Olive is perceived as a Mediterranean plant that is classified under *Oleaceae* family. It is widely found across the regions of South-East Europe, North-East Africa, and The Arabian Peninsula [9]. The growing interest in the use of natural fibers leads to consider the olive wood flour (OWF) as a substance of major ecological and economic interests. Tunisia is one of the first producers and exporters of olive oil in the region with more than 1.8 million hectares of olive trees cultivated in 2014. In addition, the olive wood used for the manufacture of handicraft products generates large quantities of wastes composed of cellulose and lignin as the main elements [10].

Attention is focused on the use of wood flour or wood dust fibers and agro-wastes [11, 12] in WPC formulations since they are renewable, lightweight, low cost, eco-friendly, and display very good mechanical properties. Softwood is an important category of wood used in the sector; it includes pine, spruce, and fir [13]. The effects of different species and wood types (heartwood and sapwood) were studied in the literature. Migneault et al. [14] compared many species of sawmill sawdust like aspen, birch, and spruce. They found that aspen as hardwood brought the highest thermal stability and stiffness to the WPC. The same tendency was observed for hard wood (white oak, black locust, and poplar) [15]. Olive wood sawdust is among the hard wood type. It has an average density of 0.81 and a higher dimensional stability, and it was an alternative for use in products that are daily exposed to external conditions. However, to the best of our knowledge there is a lack of studies focused on the olive wood plastic composites [16–18].

The mechanical strength of the WPC depends on a number of factors including nature as well as origin and species of wood. The compositions of wood could influence

the adhesion with the polymer and the effectiveness of the commercial coupling agents and modifiers. The choice of adequate treatment will not be easy as it depends on many factors. Many research works have been focused on the improvement of the compatibility and interface between matrix and fibers through the use of chemical [19, 20], physical [21], thermal [22], and enzymatic treatment of the fibers [23, 24] or use of compatibilizers during the process [4].

Amino-silane treatments, especially c-aminopropyltriethoxysilane (APS) of natural and wood fibers have been practiced extensively for decades and judged the most used with PP [25]. Amino-silane has bifunctional groups which may, respectively, react with wood fibers and PP polymer thereby forming a bridge in between them.

Heat treatments are also eco-friendly and are used to improve compatibility between polymer matrix and natural fiber. Heating wood fiber leads to modification in its chemical and physical properties. It was reported that thermal modification of wood fiber resulted in decomposition of hemicelluloses and lignin, which meant less hydroxyl group and more carbon–carbon double bonds [22, 26]. This led to an improvement of the thermal stability of the fibers and tensile strength of the composites. Aydemir et al. [27] found that the addition of heat-treated wood flour to PP matrix improved crystallinity, tensile strength, and even impact strength of the composites.

Maleic anhydride grafted polypropylene (MAPP) is an additive coupling agent that was added in the process. It is well known as an effective compatibilizer for WPC composites [28, 29]. While it develops a reaction with the hydroxyl groups in the surface of lignocellulosic fibers, MAPP diffuses to PP matrix through entanglement. In some conditions, MAPP could be more effective than alkalization and heat treatment [30]. However, the esterification reaction with the fibers depends on the composition and the fibers cell wall [31]. Since the esterification reaction between MAPP and fibers depends on the polar sites of fibers [32], many treatments or pretreatments of the fibers could enhance the reaction. Thus, many research works proceeded by co-modifications to enhance the activity of the coupling agent, citing enzymatic pretreatment [33], and alkaline pretreatment [34]. Cui et al. [35] prepared WPC with recycled HDPE using co-modifications; they found that the combination of alkali and silane treatments, in addition to MAPP, improved mechanical strength of WPC. Wang et al. [36] found that the strongest interfacial adhesion between jute fibers and recycled polypropylene was obtained when jute fibers were treated by combining alkali, silane, and MAPP treatments.

The main objective of this work was to explore the potential of olive wood flour in preparation of WPCs and to focus on an effective treatment for OWF with a promising effect on both tensile and impact strength of WPC.

Experimental

Materials

Polypropylene used in this work was a PPH 9020, a clarified homopolymer with a melt flow index (230 °C/2.16 kg) of 25 g/min was obtained from Total Petrochemicals (Belgium). The MAPP maleic anhydride (OREVAC® CA100/CA100N) was supplied from Arkema (France); it has a melt index of (190 °C / 0.325 kg) 10 g/10 min.

Fiber preparation

The olive wood fibers (OWF) comes from the region of Sfax in central Tunisia. It is recovered from wood waste generated during artisan work using a vacuum cleaner. It is then sieved and stored in plastic bags to protect it from moisture. Figure 1 shows the distribution of particles sizes of the used OWF that were in the range 52.63 µm and 111 µm.

γ-Aminopropyltriethoxysilane (APS, 99%, Sigma–Aldrich, Germany) was used for the chemical treatment of OWF through the following procedure: APS was dissolved into a solution of de-ionized water/ethanol (40/60), the mass fraction percentage of silane/OWF was 5%. Glacial acetic acid was added to the solution to adjust the pH value to 3–4. The silane solution was then coated onto the surface of the OWF at 5% of the weight of the wood fibers and parched at 105 °C for 24 h in a drying oven [10]. Using an electric oven, the heat treatment was carried out at atmospheric pressure in the presence of air and water vapor. It was conducted at 200 °C for 2 h. After pretreatment, OWF was cooled to ambient temperature. The untreated, heat-treated and silane-treated OWF samples were denoted (UOWF), (HOWF), and (SOWF), respectively.

The surfaces of fibers were also analyzed with attenuated total reflection Fourier transform infrared spectroscopy (ATR-FTIR) in a VERTEX 70 (Germany). Scans were

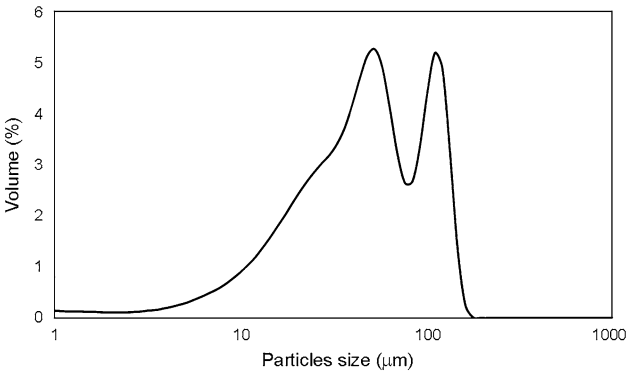

Fig. 1 Particle size distribution of OWF

run at a resolution of 4 cm^{-1}. Each specimen was scanned between 4000 and 500 cm^{-1}consisted of 100 scans recorded in absorbance units.

Using a Perkin Elmer Pyris-1 analyzer (USA), thermal gravimetric analysis (TGA) measurements were carried out on samples of about 10 mg. The temperature range used to scan the samples under nitrogen was from room temperature to 800 °C at a heating rate of 10 °C/min.

Composite preparation

The process of fabricating PP/OWF composites is shown in Fig. 2. The UOWF, HOWF, SOWF and PP samples were dried in an oven at 105 °C for 24 h prior to processing. Using a Haake internal mixer (Haake Rheomix, Thermo-Fisher Scientific, Germany), the compounding was made by measuring the process temperature in real time. The rotor speed was set at 60 rpm and the temperature at 180 °C. The internal mixer consists of a tank with a capacity of 300 cc and twin rotating blades. The tank was filled with 125 g of material, i.e. a filling rate close to 70%, which is an optimal value for the elaboration of thermoplastics.

When the MAPP and polymer seemed well melted, 30 wt% of OWF was appended to the mixer. MAPP was fixed at 2 wt%. With different treatments (PP/UOWF, PP/HOWF, PP/SOWF, PP/MAPP/HOWF, PP/MAPP/SOWF, and PP/MAPP/HOWF), the PP/OWF compounds were granulated using a RETSCH SM300 grinder (Germany) with a bottom sieve whose aperture size was 8 mm (Fig. 2). The purpose of grinding was to prepare the particles recovered from the internal mixer for injection. Thus, the particles were introduced directly into the upper part of the crusher, they are then crushed by the knives at 1500 rpm until they were large enough to pass through the bottom sieve.

Before being injected molded into $ISO^{1/2}$ test specimens, the ground particles (6 mm) were dried at 105 °C for 24 h in an oven. All ground was molded using a mini injection machine from Zamak (Poland) barrel temperature of 180 °C and a 4 bar pressure.

SEM observations were investigated using an environmental scanning electron microscope Quanta FEG 200, equipped with an Oxford Inca 350, UK, energy-dispersive X-ray microanalysis (EDX) system. The fractured surfaces of tensile test specimens were coated with a fine layer of gold in a sputtering device and the micrographs were collected.

Tensile tests were conducted in a Zwick TH010 tensile machine (Germany) with a load probe of 2.5 kN. Five dog bone specimens which were designed according to the ISO 527-2 standard were used for each treatment. An extensometer was used for the measurement of the elongation (EL%). Charpy impact strength was investigated in un-notched specimen in Zwick 5102 machine (Germany). The Charpy impact test was performed to evaluate the resistance of plastics to breakage by flexural shock according to standard test method ASTM D256. The distance between spans was 62 mm, and 15 specimens were used for each test.

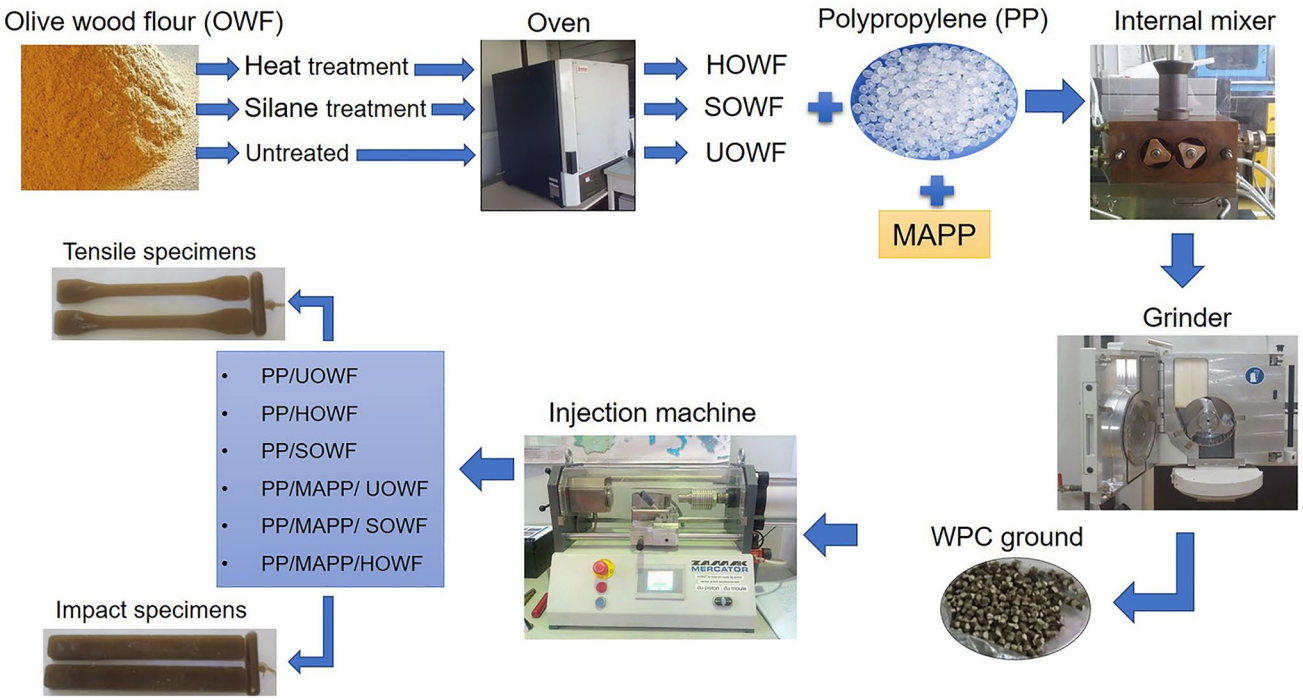

Fig. 2 Composite fabrication process

Results and discussion

Fiber characterization

The OWF samples before and after silane and heat treatments were examined with FTIR spectroscopy which their spectra are shown in Fig. 3. Table 1 summarizes the assignment of FTIR bands. The assignment of each band was identified. Only silane treatment had a remarkable effect. However, heat treatment did not have any significant effect.

The transmittance bands in the spectrum of OWF were associated with hemicellulose, cellulose, lignin, and inorganic components. The spectrum of UOWF shows the presence of a broad stretching band for intermolecular bonded hydroxyl groups at 3332 cm^{-1}. The OH groups may include absorbed water, aliphatic primary and secondary alcohols found in carbohydrates and lignin. We can observe a decrease in the transmittance intensities of the hydroxyl groups (around 3322 cm^{-1}) leading to hydrophobic olive wood flour with heat treatment.

In the case of SOWF, this broad peak partially overlapped with the hydroxyl functional groups signal due to the NH_2 functional groups of silane. The fingerprint region from 600 to 1500 cm^{-1} relates primarily to cellulose and hemicelluloses. The characteristic bands of lignin are at 1506, 1592, and 1737 cm^{-1} [51].

A broad, medium intensity ester carbonyl vibration appears at 1729 cm^{-1}, which is presumed to have come from carbonyl (C–O) stretching vibration of acetyl groups in hemicelluloses. The bands around 1506 cm^{-1} can also be distinctly identified due to the aromatic C=C skeletal vibrations mainly linked to the lignin structure.

The peak at 1455 cm^{-1}, which corresponds to the aromatic skeletal vibrations in lignin, disappeared with heat and silane treatments. The peak at 1361 cm^{-1} corresponds to the methylene groups wagging vibrations. We could observe two new peaks for SOWF at 2920 and 1605 cm^{-1}. The new band presented at region 2920 cm^{-1} after silane treatment is assigned to the C–H aliphatic stretching vibration. The band located at 1605 cm^{-1} may be attributed to C=C stretching vibration of the aromatic ring of lignin. The detected peak located at 1010 cm^{-1} came from the formation of silanol from hydrolyzation of silane groups reacting with the hydroxyl groups of the OWF. Finally, the peak at 815 cm^{-1} observed for SOWF corresponds to Si–C stretching vibration indicated that APS was attached to OWF.

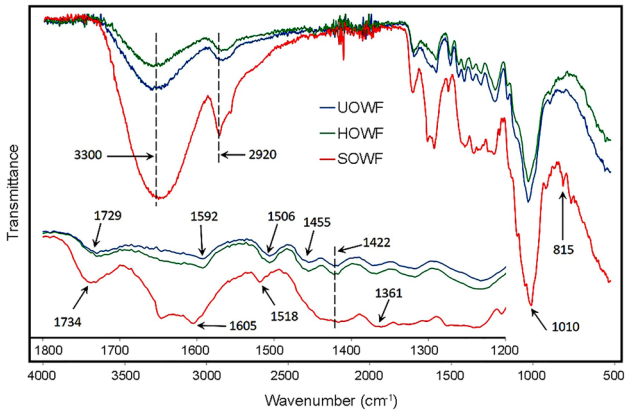

Fig. 3 FTIR spectra of UOWF, HOWF, and SOWF samples

Table 1 Assignment of FTIR observed bands for UOWF, HOWF, and SOWF samples

Wavenumber (cm^{-1})	Band assignments	Refs	UOWF	HOWF	SOWF
3300–3700	–OH stretching	[37, 38]	3332	3322	3294
2920	C–H aliphatic stretching	[37]	–	–	2920
2900	C–H and $–CH_2$-stretching of methylene and methyl group	[39]	2903	2909	–
1734	Non-conjugated C=O stretching vibration (lignin)	[40]	–	–	1737
1729	–COOH(C=O) free carboxyl groups stretching of acetyl or carboxylic acid (hemicelluloses)	[41]	1729	1730	–
1605	C=C aromatic ring of lignin	[42]	–	–	1605
1595	Aromatic skeletal vibration (lignin)	[43]	1592	1592	–
1505	C=C aromatic ring of lignin	[44]	1506	1506	1518
1456	Aromatic skeletal vibration (lignin)	[45]	1455	–	–
1422	Aromatic skeletal vibration (lignin)	[39, 46]	1422	1417	1417
1360	Methyl groups wagging vibrations	[47]	–	–	1361
1316	CH_2 wagging	[44]	1317	1317	–
1232–1246	C–O stretch in cellulose	[48]	1233	1231	1241
1032	C–O deformation in cellulose	[49]	1029	1027	1010
815	CH_2 rocking mixed with Si–C	[50]	–	–	815

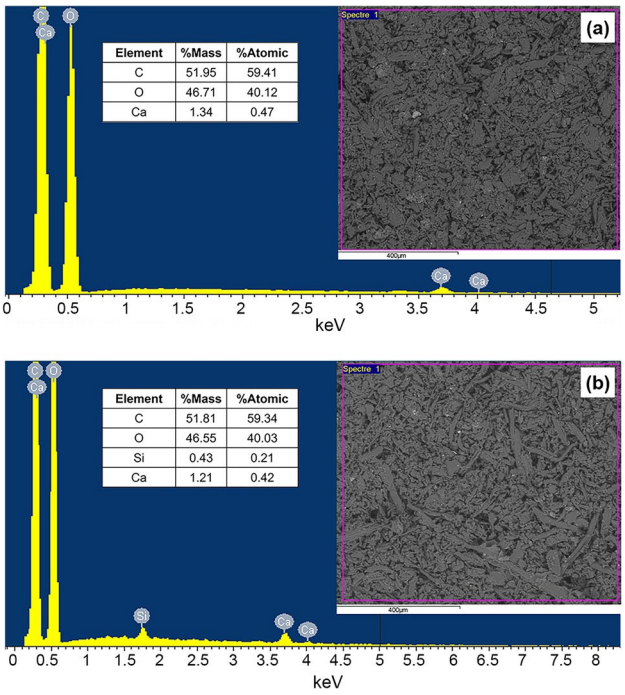

Fig. 4 SEM micrographs and EDX spectra of **a** UOWF and **b** SOWF samples

SEM micrographs and EDX spectra of UOWF and SOWF are shown in Fig. 4. The EDX analysis was performed to confirm the attachment of APS to OWF. Their EDX spectra reveal the presence of a peak corresponding to 0.43% of Si. Considering a 5% of silane in OWF, and 13% of Si in silane, the calculated percentage of Si in OWF was 0.65%, thus confirmed the attachment of APS to OWF.

Figures 5 and 6 show the TGA and DTGA curves for the untreated and treated olive wood flour specimens, respectively. For UOWF and SOWF specimens, TGA curves were associated with three stages of mass loss. Below 100 °C, the relatively small DTG peak can be assigned to the release of water (humidity, moisture) or other volatiles from the wood structures which exhibited the first initial loss. The peaks in the range of 150–375 °C, 275–350 °C, and 250–500 °C correspond to the decomposition of the hemicellulose, cellulose and lignin components [52] in OWF, respectively. The TGA curve of SOWF fibers was shifted to the right. Thus, both temperatures of the second and third peaks were increased.

Regarding the silane treatment, the temperature of a 10% loss, *T10*, was 265.04 °C which increased beyond 27 °C. The second peak corresponding to the degradation of hemicellulose increased due to the treatment as a result of the covering of the hemicelluloses with silane treatment [14].

These results were consistent with previous works indicating that silane modification increased the thermal stability of the hemp fibers in comparison to the untreated fibers [53]. The TGA data of untreated, silane-treated, and

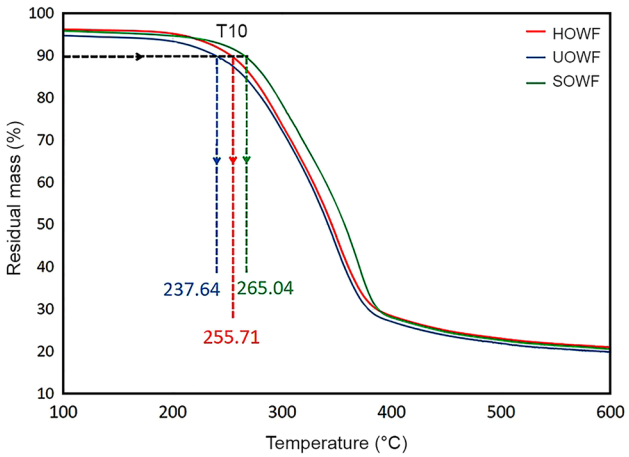

Fig. 5 TGA curves of UOWF, SOWF, and HOWF samples

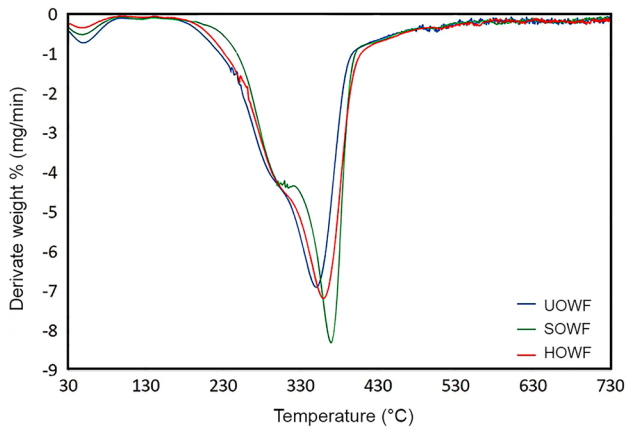

Fig. 6 DTGA curves of UOWF, SOWF, and HOWF samples

Table 2 TGA data for UOWF, SOWF, and HOWF samples

Sample code	T10	Second peak	DTG_{max}	Loss mass at 600 °C (%)
UOWF	237.64	289.43	349.7	80.09
SOWF	265.04	312.31	365.72	79.45
HOWF	255.71	291.89	352.29	78.97

heat-treated OWF samples are shown in Table 2. The third peak in DTG curve increased owing to silane treatment from 349.7 to 365.72 °C, and the weight loss decreased from 80.09 to 79.45% as a result of cellulose interaction with silane groups. Therefore, the thermal stability of OWF was improved with silane treatment due to the building of a covering layer on the cell wall between silane molecules with the cellulose and hemicelluloses [54]. We could notice

that the ash content increased as well. Thus, silane prevented the breakdown of the molecular structure of the fibers and enhanced their thermal resistances at high temperatures [55].

With respect to HOWF, we could observe that in the first stage of thermal degradation during the dehydration process from room temperature up to 220 °C, the mass loss was reduced. In fact, most hydrophilic compounds were mainly affected by the heat treatment, especially those that belong to hemicelluloses submitted to dehydration reaction with the destruction of hydroxyl groups. Therefore, HOWF has a lower water affinity and consequently better dimensional stability [56].

The heat treatment increased *T10*, DTG_{max}, and ash content of HOWF because of the degradation of hemicelluloses and condensation of lignin [26]. Heat treatment enhanced the thermal resistance of the OWF. Both treatments enhanced the thermal resistance of the OWF that could also improve the thermal stability of the composites.

Concerning HOWF sample, we could observe that in the first stage of thermal degradation during the dehydration process from room temperature up to 220 °C, the mass loss was reduced with the increase of treatment temperature. In fact, most hydrophilic compounds were mainly affected by heat treatment, especially those that belong to hemicelluloses submitted to dehydration reaction with the destruction of hydroxyl groups. Therefore, HOWF sample showed a lower water affinity and consequently better dimensional stability [56]. The heat treatment increased both *T10* and ash content of HOWF as a result of degradation of hemicelluloses and condensation of the lignin. This result was in line with the previous works of Aydemir et al. [57].

Composite characterization

The tensile tests made it possible to determine the variation of the Young's modulus for each treatment as shown in Fig. 7. Adding MAPP to PP decreased Young's modulus from 1866 to 1596 MPa. This is related to the lower elasticity of MAPP. The addition of the MAPP compatibilizer in the composites does not show a significant difference. In fact, it was reported [4] that, for the stiffness, the effects of MAPP compatibilization were less pronounced. Moreover, as stiffness behavior was calculated for lower deformation, the effect of interfacial interaction was not more significant than the effect of the aspect ratio of wood flour dispersion and processing defects.

A similar effect of silane treatment was reported in the previous works of Rojo et al. [54]. The combination of MAPP and silane treatments enhanced the stiffness of the samples compared to PP/MAPP/UOWF and PP/MAPP/HOWF composites; this may be due to good dispersion of the fibers in the matrix.

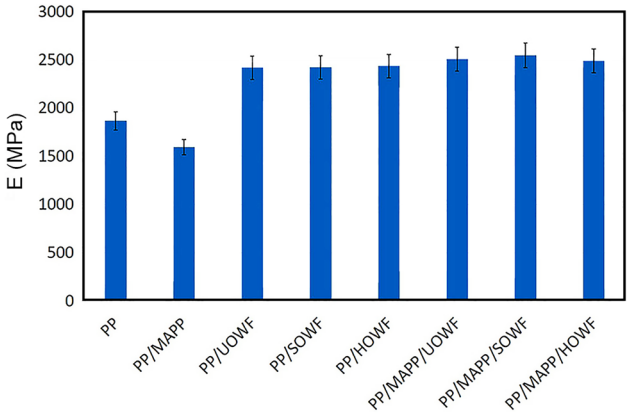

Fig. 7 Variations of the Young's modulus as functions of different treatments

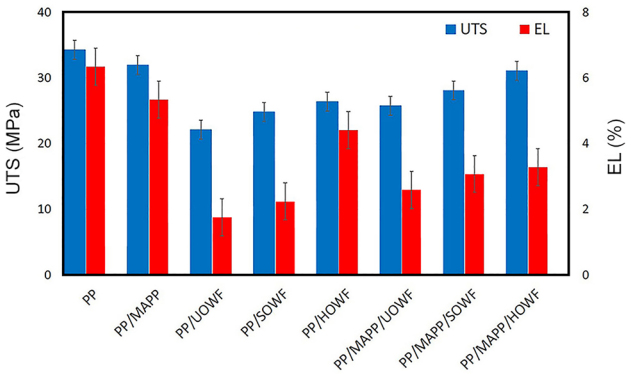

Fig. 8 Variations of UTS and EL (%) for different treatments

Figure 8 shows the ultimate tensile strength (UTS) and the elongation of elaborated composites with different surface modifications. The tensile strength of 30 wt% OWF WPC decreased from 34 ± 1.5 MPa to 23 ± 0.6 MPa. As can be observed, the UTS of the PP/SOWF, PP/HOWF, PP/MAPP/UOWF, PP/MAPP/SOWF, and PP/MAPP/HOWF composites were improved by 10.8%, 16.2%, 14.2%, 21.3%, and 28.8%, respectively, compared with that of the untreated PP/UOWF composite. This increase in UTS may be an outcome of the improved interfacial adhesion between OWF and matrix.

Silane modification enhanced the tensile strength. This is due to better adhesion with the APS [25]. Higher interfacial adhesion leads to better transfer of stress between wood flour and polymer. First, by forming a chemical bond with the organic functional groups bonded to PP, silane molecules acted as a link between the wood flour and matrix. Second, with some of the hydroxyl groups on the fibers surface, wood flour react with the hydroxyl groups of silanol (obtained after hydrolysis of silane). The further addition of MAPP leads to more interaction with fibers through the

reaction of hydroxyl groups in OWF. As a result, polarity decreased and the compatibility was improved.

The PP/MAPP/HOWF composites exhibited higher tensile strength, thus heat treatment of OWF enhanced the activity of MAPP. In fact, the heat treatment helped decomposition of hemicelluloses and lignin on the surface of OWF, release acetic acid and increase cross-linking in the lignin–carbohydrate complex [57], which promoted the action of MAPP.

The effect of different treatments of OWF on the elongation of WPCs is shown in Fig. 8; surprisingly we could observe a little increase of elongation-at-break in samples for all the treatments. This may be due to the plastic deformation of the matrix between the fibers and the enhancement of the fibers dispersion after treatment. The heat treatment of the fibers in particular seems to be the most efficient method for improving the composites ductility and toughness.

The mechanical properties of these blends are closely related to their morphology and wettability between PP and OWF. SEM observations (Fig. 9) of fractured surface of tensile test specimens for the PP-based composites reinforced with OWF were also carried out to investigate the fiber–matrix interfaces and compare their aspects after different treatments. The fractured surface for PP/UOWF composite shown in Fig. 9a is characterized by a brittle surface with much porosity. It is clear that the interfacial adhesion between the fibers and matrix was weak. However, in the case of the PP/MAPP/UOWF composite (Fig. 9b), we could observe the pullout of the fibers, the debonding between the fibers and matrix. When using silane treatment (Fig. 9c), there is a mixture of fractures modes (brittle and ductile). Compared to the untreated fibers, the treatment with silane improved slightly the adhesion in the interfacial region as indicated by the breakage of the fibers and by the absence of any physical contact between both components. In the case of the PP/HOWF fractured surface, Fig. 9d shows the breakage of the fibers due to good adhesion between fibers and matrix; this was in accordance with the higher elongation-at-failure. Likewise, no discontinuity was reported between the two phases and the fibers seem to be totally layered by the matrix. This observation yields direct evidence about the adhesion improvement at the interface in the presence of HOWF.

Figure 10 shows the results of Charpy impact tests of the WPC composites. The addition of MAPP to PP increased the impact strength of material by 31%. However, the addition

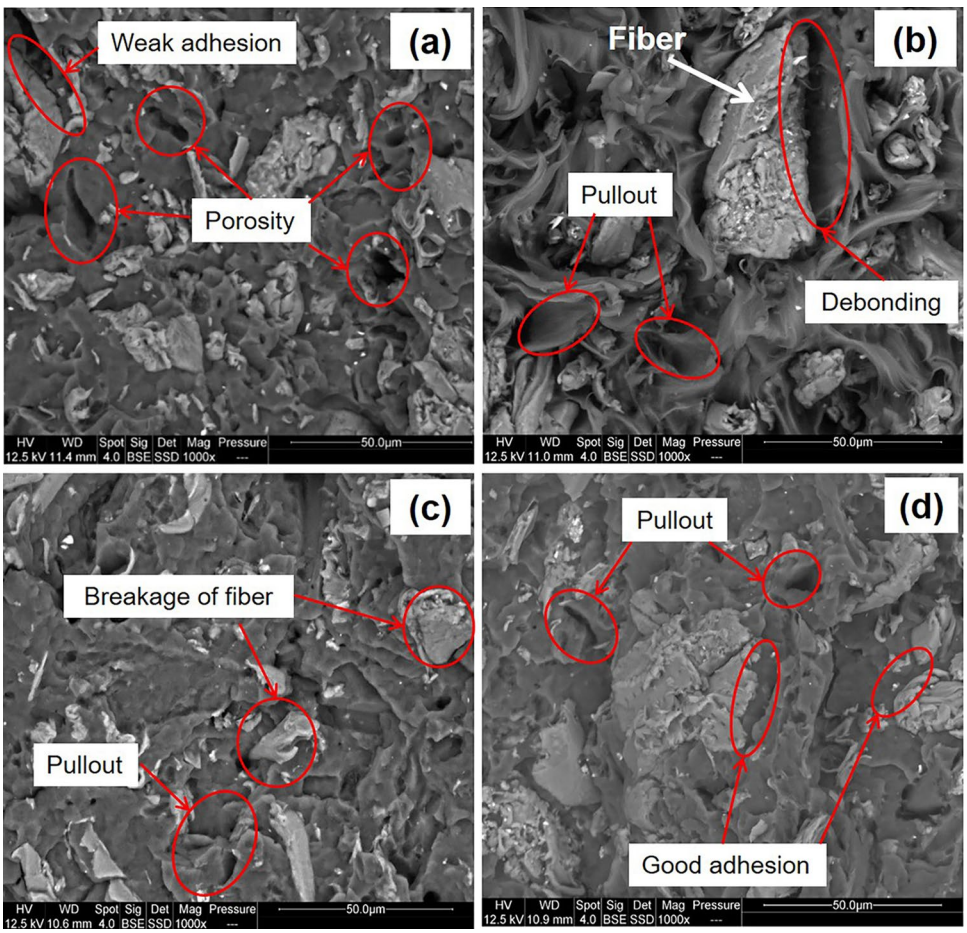

Fig. 9 SEM micrographs of fractured surfaces of PP-based composites reinforced with **a** UOWF, **b** MAPP/UOWF, **c** SOWF, and **d** HOWF

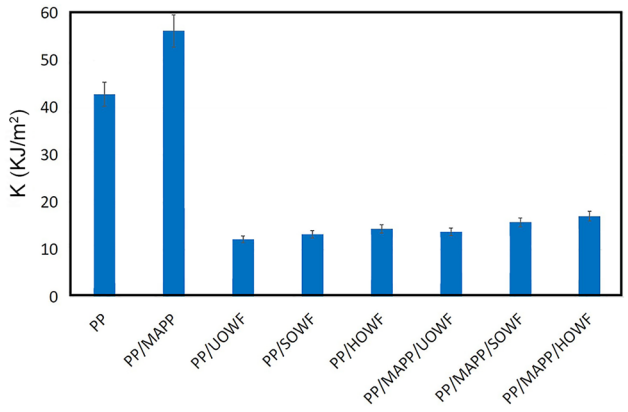

Fig. 10 Variations of Charpy impact energy for different treatments

of OWF to PP matrix decreased the impact strength in PP composites when compared to neat PP. It is well known that the addition of fibers decreases the impact strength in polymers. Because, it reduces the ductility of polymers and hampers plastic deformation by restricting polymer chains [58]. The silane treatment improved impact strength. Although, the improvement was not as pronounced as expected, probably because the filler content was high, the OWF tended to form agglomerations in the PP matrix. The improvement in toughness also indicated the improved adhesion between the filler and matrix in the composite. If the addition of MAPP promoted an improvement in impact strength, it generally did not allow composites (PP/OWF) to have an acceptable resilience, even if there was an improvement in ductility and resilience. This is the reason why silane and heat treatments are necessary. It would be clear that the highest impact strength was observed with heat treatment by more than 52%; this was in accordance with the increase of the toughness.

Compared to the original WPC, the silane-treated fibers decreased the impact strength of the WPCs. According to Sobczak et al. [4], the effect of the silane on the impact strength was ambiguous. Normally, they would decrease the impact strength. Combination of the MAPP as a compatibilizer and the heat treatment led to the improvement of the impact strength of the WPCs. This is in accordance with the ductile behavior observed in tensile properties.

Conclusion

The effects of the silane and heat treatments of OWF and use of MAPP compatibilizer were studied on the interfacial adhesion of the PP/OWF composites. The components of the PP/OWF composites generated imperfect adhesion between themselves. Silane and heat treatment improved the thermal stability of OWF. Single treatments (silane or heat treatments) did not lead to a better enhancement of the mechanical strength of these composites. The co-modification of silane treatment with MAPP enhanced the effectiveness of the MAPP activity for the fibers. Furthermore, the co-modification with heat treatment is a promising eco-friendly treatment since it improved not only the interfacial adhesion but also ductility and impact strength of these composites. The remarkable finding was the increase of the ductility in the case of the MAPP and heat treatment.

Acknowledgements The authors are grateful to the Polymers, Composites, and Hybrids (PCH) team of the Materials Center of IMT Mines Alès (C2MA), France for donating the necessary raw materials and instruments. They would also like to thank Dr. H. Souissi (Assistant Professor of English language at Imam Ibn Saud Islamic University) for a grant support to edit the language for this paper.

Declarations

Conflict of interest The authors declare that they have no conflict of interest.

References

1. Xiao F, Zhu L, Yu L (2020) Evaluation of interfacial compatibility in wood flour/polypropylene composites by using dynamic thermomechanical analysis. Polym Compos 41:3606–3614
2. Wang W, Chen H, Li J (2021) Effects of maleic anhydride grafted polypropylene on the physical, mechanical and flammability properties of wood-flour/polypropylene/ammonium polyphosphate composites. Fibers Polym 22:1137–1144
3. Asim M, Paridah MT, Chandrasekar M, Shahroze RM, Jawaid M, Nasir M, Siakeng R (2020) Thermal stability of natural fibers and their polymer composites. Iran Polym J 29:625–648
4. Sobczak L, Brüggemann O, Putz RF (2013) Polyolefin composites with natural fibers and wood-modification of the fiber/filler-matrix interaction. J Appl Polym Sci 127:1–17
5. La Mantia FP, Morreale M (2008) Accelerated weathering of polypropylene/wood flour composites. Polym Degrad Stabil 93:1252–1258
6. Gremmel-Simon H, Fachhochschule Burgenland (2016) Nachhaltige Technologien: Gebäude--Energie--Umwelt: Internationaler Kongress e-nova 2016, 24 und 25 November 2016, Band 20. Leykam, Graz
7. Ilyas RA, Sapuan SM (2020) Biopolymers and biocomposites: chemistry and technology. CAC 16:500–503
8. Chandrasekar M, Ishak MR, Jawaid M, Sapuan SM, Leman Z (2018) Low velocity impact properties of natural fiber-reinforced composite materials for aeronautical applications. In: Jawaid M (ed) Sustainable composites for aerospace applications. Elsevier, Amsterdam
9. Kian LK, Saba N, Jawaid M, Alothman OY, Fouad H (2020) Properties and characteristics of nanocrystalline cellulose isolated from olive fiber. Carbohydr Polym 241:116423
10. Bouhamed N, Souissi S, Marechal P, Amar MB, Lenoir O, Leger R, Bergeret A (2020) Ultrasound evaluation of the mechanical properties as an investigation tool for the wood-polymer composites including olive wood flour. Mech Mater 148:103445
11. Haddar M, Elloumi A, Koubaa A, Bradai C, Migneault S, Elhalouani F (2018) Synergetic effect of *Posidonia oceanica* fibres

and deinking paper sludge on the thermo-mechanical properties of high density polyethylene composites. Ind Crops Prod 121:26–35
12. Bekhta P, Sedliačik J, Kačík F, Noshchenko G, Kleinová A (2019) Lignocellulosic waste fibers and their application as a component of urea-formaldehyde adhesive composition in the manufacture of plywood. Eur J Wood Prod 77:495–508
13. Bledzki AK, Franciszczak P, Osman Z, Elbadawi M (2015) Polypropylene biocomposites reinforced with softwood, abaca, jute, and kenaf fibers. Ind Crops Prod 70:91–99
14. Migneault S, Koubaa A, Perré P (2014) Effect of fiber origin, proportion, and chemical composition on the mechanical and physical properties of wood-plastic composites. J Wood Chem Technol 34:241–261
15. Fabiyi JS, McDonald AG (2010) Effect of wood species on property and weathering performance of wood plastic composites. Compos Part A Appl Sci Manuf 41:1434–1440
16. Abdellah Ali SF, Althobaiti IO, El-Rafey E, Gad ES (2021) Wooden polymer composites of poly(vinyl chloride), olive pits flour, and precipitated bio-calcium carbonate. ACS Omega 6:23924–23933
17. Jawaid M, Awad S, Fouad H, Alothman OY, Saba N, Sain M, Leao AL (2022) Olive cellulosic fibre based epoxy composites: thermal and dynamic mechanical properties. J Nat Fibers. https://doi.org/10.1080/15440478.2022.2053266
18. Sarmin SN, Jawaid M, Awad SA, Saba N, Fouad H, Alothman OY, Sain M (2022) Olive fiber reinforced epoxy composites: dimensional stability, and mechanical properties. Polym Compos 43:358–365
19. Siakeng R, Jawaid M, Tahir PMd, Siengchin S, Asim M (2020) Improving the properties of pineapple leaf fibres by chemical treatments. In: Jawaid M, Asim M, Tahir PMd, Nasir M (eds) Pineapple leaf fibers. Springer Singapore, Singapore
20. Orue A, Jauregi A, Peña-Rodriguez C, Labidi J, Eceiza A, Arbelaiz A (2015) The effect of surface modifications on sisal fiber properties and sisal/poly (lactic acid) interface adhesion. Compos B Eng 73:132–138
21. Li Y, Zhang J, Cheng P, Shi J, Yao L, Qiu Y (2014) Helium plasma treatment voltage effect on adhesion of ramie fibers to polybutylene succinate. Ind Crops Prod 61:16–22
22. Kaboorani A, Faezipour M, Ebrahimi G (2008) Feasibility of using heat treated wood in wood/thermoplastic composites. J Reinf Plast Compos 27:1689–1699
23. Werchefani M, Lacoste C, Elloumi A, Belghith H, Gargouri A, Bradai C (2020) Enzyme-treated Tunisian alfa fibers reinforced polylactic acid composites: an investigation in morphological, thermal, mechanical, and water resistance properties. Polym Compos 41:1721–1735
24. George G, M, Mussone PG, Alemaskin K, Chae M, Wolodko J, Bressler DC, (2016) Enzymatically treated natural fibres as reinforcing agents for biocomposite material: mechanical, thermal, and moisture absorption characterization. J Mater Sci 51:2677–2686
25. Nachtigall SMB, Cerveira GS, Rosa SML (2007) New polymeric-coupling agent for polypropylene/wood-flour composites. Polym Test 26:619–628
26. Kaboorani A (2009) Thermal properties of composites made of heat-treated wood and polypropylene. J Compos Mater 43:2599–2607
27. Aydemir D, Alsan M, Altuntas E, Oztel A (2019) Mechanical, thermal and morphological properties of heat-treated wood-polypropylene composites and comparison of the composites with PROMETHEE method. Plast Rubber Compos 48:389–400
28. Arbelaiz A, Fernández B, Cantero G, Llano-Ponte R, Valea A, Mondragon I (2005) Mechanical properties of flax fibre/polypropylene composites. Influence of fibre/matrix modification and glass fibre hybridization. Compos Part A Appl Sci Manuf 36:1637–1644
29. Bledzki AK, Faruk O (2004) Creep and impact properties of wood fibre–polypropylene composites: influence of temperature and moisture content. Compos Sci Technol 64:693–700
30. Kaewkuk S, Sutapun W, Jarukumjorn K (2013) Effects of interfacial modification and fiber content on physical properties of sisal fiber/polypropylene composites. Compos B Eng 45:544–549
31. Bouafif H, Koubaa A, Perré P, Cloutier A, Riedl B (2008) Analysis of among-species variability in wood fiber surface using DRIFTS and XPS: effects on esterification efficiency. J Wood Chem Technol 28:296–315
32. Migneault S, Koubaa A, Perré P, Riedl B (2015) Effects of wood fiber surface chemistry on strength of wood–plastic composites. Appl Surf Sci 343:11–18
33. Li X, Xiao R, Morrell JJ, Wu Z, Du G, Wang S, Zou C, Cappellazzi J (2018) Improving the performance of bamboo and eucalyptus wood fiber/polypropylene composites using pectinase pre-treatments. J Wood Chem Technol 38:44–50
34. Dominkovics Z, Dányádi L, Pukánszky B (2007) Surface modification of wood flour and its effect on the properties of PP/wood composites. Compos Part A Appl Sci Manuf 38:1893–1901
35. Cui Y, Lee S, Noruziaan B, Cheung M, Tao J (2008) Fabrication and interfacial modification of wood/recycled plastic composite materials. Compos Part A Appl Sci Manuf 39:655–661
36. Wang X, Cui Y, Xu Q, Xie B, Li W (2010) Effects of alkali and silane treatment on the mechanical properties of jute-fiber-reinforced recycled polypropylene composites. J Vinyl Addit Technol 16:183–188. https://doi.org/10.1002/vnl.20230
37. Es-haghi H, Mirabedini SM, Imani M, Farnood RR (2014) Preparation and characterization of pre-silane modified ethyl cellulose-based microcapsules containing linseed oil. Colloids Surf A Physicochem Eng Asp 447:71–80
38. Karabacak M, Kurt M, Çınar M, Çoruh A (2009) Experimental (UV, NMR, IR and Raman) and theoretical spectroscopic properties of 2-chloro-6-methylaniline. Mol Phys 107:253–264
39. Meng F, Yu Y, Zhang Y, Yu W, Gao J (2016) Surface chemical composition analysis of heat-treated bamboo. Appl Surf Sci 371:383–390
40. Sobral Hilário L, Batista dos Anjos R, de Moraes B, Juviniano H, da Silva DROD (2019) Evaluation of thermally treated *Calotropis procera* fiber for the removal of crude oil on the water surface. Materials 12:3894
41. Rosu D, Teaca C-A, Bodirlau R, Rosu L (2010) FTIR and color change of the modified wood as a result of artificial light irradiation. J Photochem Photobiol B 99:144–149
42. Srisuwan L, Jarukumjorn K, Suppakarn N (2018) Effect of silane treatment methods on physical properties of rice husk flour/natural rubber composites. Adv Mater Sci Eng 2018:1–14
43. Zhuang J, Li M, Pu Y, Ragauskas A, Yoo C (2020) Observation of potential contaminants in processed biomass using Fourier transform infrared spectroscopy. Appl Sci 10:4345
44. Åkerholm M, Salmén L (2001) Interactions between wood polymers studied by dynamic FT-IR spectroscopy. Polymer 42:963–969
45. Chen Y, Tshabalala MA, Gao J, Stark NM, Fan Y (2014) Color and surface chemistry changes of extracted wood flour after heating at 120 °C. Wood Sci Technol 48:137–150
46. Yu J, Ramirez Reina T, Paterson N, Millan M (2022) On the primary pyrolysis products of torrefied oak at extremely high heating rates in a wire mesh reactor. Appl Energy Combust Sci 9:100046
47. Wondu E, Lule ZC, Kim J (2020) Fabrication of aliphatic water-soluble polyurethane composites with silane treated $CaCO_3$. Polymers 12:747
48. Chen Z, Hu TQ, Jang HF, Grant E (2015) Modification of xylan in alkaline treated bleached hardwood kraft pulps as classified

by attenuated total-internal-reflection (ATR) FTIR spectroscopy. Carbohyd Polym 127:418–426
49. Azizan A, Jusri NAA, Azmi IS, Abd Rahman MF, Ibrahim N, Jalil R (2022) Emerging lignocellulosic ionic liquid biomass pretreatment criteria/strategy of optimization and recycling short review with infrared spectroscopy analytical know-how. Mater Today Proc 63:S359–S367
50. Tee YB, Talib RA, Abdan K, Chin NL, Basha RK, Yunos KFM (2013) Thermally grafting aminosilane onto kenaf-derived cellulose and its influence on the thermal properties of poly(lactic acid) composites. BioResources 8:4468–4483
51. Popescu C-M, Popescu M-C, Singurel G, Vasile C, Argyropoulos DS, Willfor S (2007) Spectral characterization of eucalyptus wood. Appl Spectrosc 61:1168–1177
52. Verheyen S, Blaton N, Kinget R, Kim H-S (2004) Thermogravimetric analysis of rice husk flour filled thermoplastic polymer composites. J Therm Anal Calorim 76:395–404
53. Lu N, Oza S (2013) Thermal stability and thermo-mechanical properties of hemp-high density polyethylene composites: effect of two different chemical modifications. Compos B Eng 44:484–490
54. Rojo E, Alonso MV, Oliet M, Del Saz-Orozco B, Rodriguez F (2015) Effect of fiber loading on the properties of treated cellulose fiber-reinforced phenolic composites. Compos B Eng 68:185–192
55. Kabir MM, Wang H, Lau KT, Cardona F (2013) Effects of chemical treatments on hemp fibre structure. Appl Surf Sci 276:13–23
56. Shen DK, Gu S, Bridgwater AV (2010) The thermal performance of the polysaccharides extracted from hardwood: cellulose and hemicellulose. Carbohydr Polym 82:39–45
57. Aydemir D, Kiziltas A, Erbas Kiziltas E, Gardner DJ, Gunduz G (2015) Heat treated wood–nylon 6 composites. Compos B Eng 68:414–423
58. Ogunsona EO, Misra M, Mohanty AK (2017) Sustainable biocomposites from biobased polyamide 6,10 and biocarbon from pyrolyzed miscanthus fibers. J Appl Polym Sci 134:44221